Graphite nanoplatelets filled silicone composites with novel electrical and dielectric properties

Renaud Metz, Christophe Blanc, Guillaume Prevot, Mehrdad Hassanzadeh

Graphite Nanoplatelets Filled Silicone Composites with Novel Electrical and Dielectric Properties

Renaud Metz[1,2], Christophe Blanc[1], Guillaume Prévost[1], Mehrdad Hassanzadeh[3]

[1]Laboratoire Charles Coulomb UMR 5221 CNRS-Université de Montpellier, Place Eugène Bataillon, Bâtiment 11, Montpellier, France

[2]Université Claude Bernard - Lyon 1, Villeurbanne, France

[3]Schneider Electric, 37 Quai Merlin, 38000 Grenoble, France

Keywords: graphite nanoplatelets, nonlinear composite material, field grading material

Address correspondence to E-mail: Renaud.metz@gmail.com

Abstract

In the design of medium and low voltage equipment such as cable accessories, generator, motor end windings or bushings, issues with electrical field enhancement occur at interfaces between insulators and conductors, resulting in accelerated material ageing. The purpose of this paper is to present a novel dielectric composite material which has the properties to mitigate this local amplification. It is a functional dielectric which resistivity decreases by several orders with electric field from 10^{14} to 10^{9} Ωm up to 1 kVmm^{-1} while the dielectric constant decreases from 15 to 12 in the 10^{-2} – 10^{6} Hz range. This novel material is made with graphite nanoplatelets. It may be used as a resistive or capacitive field grading material in electrical applications.

1 Introduction

The increasing energy demand with the concomitant decrease of the size of the electric devices and the penetration of renewable energy sources such as wind farms and solar power systems in the distribution network, imply additional electric stress on voltage insulating materials [1–10]. Providing an efficient and safe insulation is therefore a challenge. As a matter of fact, intense electric fields can generate localized partial discharges, resulting in accelerated aging

or even dielectric breakdown. Electrical system design is therefore optimized to prevent or limit any intensification of the electric field at “triple points” or “triple junctions” (where three materials with different permittivity meet) [1-2]. A classical way to highlight the triple points problem consists to consider the essential components of a cable: a conductor, an insulator and a ground shield. At cable termination where the shield has been removed, the electric field concentrated in the insulation is spread out (**Fig. 1. A**). A concentration of voltage equipotential lines is observed at the triple point where the interfaces between the shield, the insulator and the air meet. In **Fig. 1. B**, the triple point has been coated with a material that has a high enough dielectric constant to redistribute AC fields, i.e. make the voltage equipotential lines scatter. The optimized length and thickness of the coating depend on the specific design as such as the geometry and the detailed dielectric properties of the layers. Such a solution does grade the distribution of the potential as depicted in Fig.1.B. There also exist capacitive field grading materials that have nonlinear dielectric constant that increases with the field. These solutions do not work in DC. In order to get a coating which works under DC as well as AC and imSurge conditions, it is advantageous to use a material that possesses a nonlinear resistivity which decreases with the field. In **Fig. 2**, an overview of the different methods that are used or proposed to control the field in practice is depicted. At first and for most electrical or electronic equipment, geometric field grading (**Fig. 2.**1.) is used. It means that the design of the equipment is optimized in order to decrease the local field enhancement. The metal parts are usually bent and/or the thickness of the insulator is locally increased. This is the first choice of treatment. To decrease further the field, processing of field grading materials is carried out (**Fig.2.**2.). Those composites are made by adding to polymers inorganic filler with a specific permittivity (**Fig.2**.3.) or resistivity (**Fig.2**.4.). There is also an approach in which the insulating body is made up of a staggered arrangement of one or several concentric cylindrical layers of insulating material and layers of conducting materials. The conducting layers are insulated, with floating potential (**Fig.2** 5). For each method, the preferential AC/DC or overvoltage conditions of operation are reported. It appears that only the linear resistive field grading solution works under DC conditions but not against overvoltage (surge) that are likely to occur in the mains supply. For this, nonlinear field grading materials are necessary (**Fig.2** 6). Contrary to nonlinear capacitive field grading materials (**Fig.2** 7). The unique solution which might be used under AC, DC and surge conditions is nonlinear resistive field grading (**Fig.2.** 8). This work aims at presenting the interest of such a new nonlinear resistive field grading composite material made of graphite nanoplatelets randomly dispersed in a polymer and at evaluating its performances for medium voltage applications.

Fillers known to transfer their non-linear electric properties to the matrix of a composite mainly consist of ZnO microvaristors and/or other metallic oxides, [12-20] doped silicon carbide [21-26] or carbonaceous particles [27-32]. Among carbon fillers, nano-sheets have driven attention because nonlinear composites may be obtained at a low filling ratio (< 5 vol.%). A pioneering work was based on the study of nanocomposites made of monolayers of graphene oxide (GO) previously slightly thermally reduced [33-34]. The switching field E_s, above which there is a departure from Ohmic behavior ($\rho \propto E^{-\alpha}$, $\alpha > 1$, for $E > E_s$) was modulated not only by the nanosheet volume fraction used but also by the GO reduction rate [35,37]. The non-linear effects were then attributed to the numerous surface oxide groups of the nanosheets at the origin of barrier voltages.

Recently, Gaska *et al.* prepared nanocomposites from graphite nanoplatelets (GnP) dispersed and oriented by extrusion in low-density polyethylene [36,37]. A nonlinear behavior was observed at very high fields ~ 20MVm^{-1} (20kVmm^{-1}). This result was not expected since these fillers do not exhibit surface oxide groups comparable to the ones which decorate the surface of GO, neither in quality nor in density. Recently we retrieved this result with graphite nanoplatelets dispersed in a silicone matrix [38].

In this paper, after briefly recalling the electrical behavior of these new composites, we report a detailed characterization of their properties. In particular, we show that they reveal a fair dielectric constant increase at small filler loadings concomitant to a decrease of the resistivity with the electric field. We report the detailed electrical characteristics of the composites and consider their use for resistive and capacitive field grading. We then discuss the possible origins of the global non-linear electrical behavior.

2 Materials and method

Raw materials: The silicone matrix used in this study is the Bluestar RTV141 resin. It is a room temperature vulcanizing silicone, reticulated by poly-addition. The graphite nanoplatelets (GnP) fillers were purchased from XG Sciences in powder form. The grade M25 was carried

out in this work. According to the supplier, the mean diameter of these platelets as primary particles is around 25µm and their mean thickness around 6nm, corresponding to about 20 layers of graphene monolayers stacked on top of each other's. Our analysis by optical microscopy and secondary electron microscopy show that the nanoplatelets are not isolated from one another. They tend to gather together into disordered clusters made of entangled platelets, some dimensions of which are significantly larger than several microns. Furthermore, primary nanoplatelets form strongly bonded aggregates. Large shear forces are required to break the latter and to obtain individual nanoplatelets. Such shear forces were not carried out during the processing of our composites despite the use of a speed mixer, *i.e.* a bladeless mixer which combines dual asymmetric centrifugal mixing technology. Large micronic aggregates up to 100 µm are still observed in the final materials.

Composite Fabrication: To prepare the composites, a master batch filled with 5 wt.% of GnP was first prepared by inserting the fillers progressively in the silicone resin and manually mixing for homogenizing. The GnP fillers were then dispersed in the matrix by dual asymmetric centrifugal mixing using a Flacteck Speedmixer from Hauschild. The composites were prepared by inserting this master batch into the right amount of neat resin, and by mixing it with the help of the speed mixer. The dispersion was performed under primary vacuum (~ 400 Pa) to simultaneously degas the composite. The hardener was then added to the mixture and dispersed by the same technique. The final blend was poured in a steel open mold of 1 mm thick previously heated at T = 150°C. To ensure a full polymerization, the samples are heated during 1 hour at 150°C under 150 bars and 2 hours at 90°C during 30 minutes under 150 bars. Specimens of 110mm x 77mm x 1mm dimensions were prepared for electrical characterization by compression molding at 15MPa and then curing at 150°C during 1hour (**Fig. 3**).

Composite characterization: The chemical bonding of the composite surfaces was examined by an Attenuated Total Reflection (ATR) Fourier-transformed infrared (FT-IR) spectroscopy (Perkin Elmer, USA) in the wavelength range of 400-4000 cm^{-1}.

In the range 0-1kV, the procedure for determining the volume resistivity is based on the current absorption-resorption method according to ASTM D 257-14 [39]. A guarded cell linked to a high voltage DC power supply and picoammeter (Keithley electrometer 6517B) is used. A guard ring configuration was used for the measurements in order to exclusively evaluate volume conductivity. In this configuration, surface currents are diverted directly to ground and are thus not measured. Polarization and depolarization of a duration of 1 hour are carried out for the neat polymer matrix and of 30 minutes for the GnP-based composites (after a first polarization at 1kVmm^{-1}). Volume resistivity is calculated with the following relation: $\rho = \frac{R\,A}{h}$ where ρ is the volume resistivity in Ωm, R the measured volume resistance, in Ω, A the effective area of the guarded electrode, in m^2 and h the average thickness of the specimen. In the case of the measuring cell, the diameter of the electrode was 54 mm.

We have also measured the behavior of the sample at high field in AC (50Hz). A $\frac{\pi}{2}$ phase shift between current and voltage was observed, indicating a mainly capacitive behavior at this frequency. The dielectric permittivity ε_r (real part) was extracted from the data.

The dielectric measurements were performed on a Broadband Dielectric Spectrometer, Novocontrol alpha analyzer, using an applied ac voltage of 1V, over a frequency range from 10^{-2} Hz to 1MHz Gold electrodes on both sides of the samples were previously deposited by sputtering with a thickness of ~ 20 nm).

3 Results

3.1 FT-IR Spectroscopy

Fig. 4 shows the attenuated total reflection Fourier-transformed infrared spectra of the neat silicone rubber and the 4 wt.% filled silicone after full reticulation at 150°C. The mean peaks are Si-CH_3 at 1260 cm^{-1} and 1400 cm^{-1}, together with CH_3 peaks near 2900 cm^{-1} for side chains of silicone [40]. Both peaks around 1000-1100 cm^{-1} have been attributed to Si-O-Si and the peaks near 800 cm^{-1} to $(CH_3)_2$-Si-O groups. The spectra are very similar and suggest that

the silicone rubber was not modified by the presence of the graphite nanoplatelets. This suggests that the nanoplatelets do not take part to the chemical covalent chains of the silicone network.

3.2 Resistivity versus DC electric field

Fig. 5 shows the change of resistivity of the GnP based composite as a function of the electrical field for an increasing volume fraction of fillers. It is interesting to note that the resistivity extends over a large range of values (10^9-10^{16} Ωm). The pristine silicone resin and low filled composites (1-3 wt. %) are insulators with a resistivity in the 10^{16}- 10^{14} Ωm range and a slight rise of resistivity is observed at high electric fields. Surprisingly, these composite materials exhibit a higher resistivity than that of the pristine silicone matrix. This is not intuitive since the graphite nanoplatelets are conductive (through and in-plane resistivities: 10^{-2} and 10^{-7} Ωm^{-1}, respectively) [36]. Adding such fillers in an insulating matrix should *a priori* lead to an increase of the conductivity of the composites. However, such a macroscopic behavior has already been reported [33,42] and attributed to ionic transport disturbed by the nanoplatelets network [33], trapping of charge carriers in deep traps [41] or thought as an electronic Coulomb blockade phenomenon [42]. In contrast, the electrical behavior significantly changes for filler concentrations above 4 wt. % and is typical of that of percolated composites with $\rho = \rho_f (f - f_c)^t$, where ρ_f is the resistivity of the conductive filler, f and f_c are the actual and critical filler volume fraction respectively and t is the critical exponent of resistivity.

Fig. 6 compares the conductivity of the most loaded sample (5 wt.%) with the data from References [33-35]. The graphite nanoplatelets composite materials exhibit a switching field $\sim 3 \times 10^4 \mathrm{Vm}^{-1}$ which is two orders of magnitude lower than slightly thermally reduced graphene oxide (GO)-based nanocomposites for which $E_s \sim 10^6 \mathrm{Vm}^{-1}$ ($1 \mathrm{kVmm}^{-1}$). The GO was thermally reduced at 120°C for 12 h in dry air to obtain nonlinear properties. (As received GO-Silicone at 3 wt. is reported: such nanocomposite remains insulating even at the highest electric

field : 6.3 10^{12} Ω.m at 6 kV/mm [35]). Above this breakdown field, the resistivity behaves nonlinearly with a nonlinear coefficient $\alpha = \log\left(\frac{\rho_1}{\rho_2}\right)/\log\left(\frac{E_1}{E_2}\right) \sim 3$, lower than α~10 for slightly reduced GO-based nanocomposites. **Fig. 6** also reports the conductivity of the GnP-based extruded composite studied in the References [36-37]. The extrusion of the loaded low-density polyethylene results in the alignment of the GnP fillers. The electric conductivity has been measured perpendicularly to this direction. It is about 6 orders of magnitude lower than the parallel one. The nonlinear coefficient $\alpha \sim 4$ suggests that the orientation of the GnP does not influence the nonlinearity; only the switching field ($\sim 2 \times 10^7$ Vm^{-1}) is affected. A correlation between the nanoplatelets and the nonlinear property is however tricky since the matrix is a low-density polyethylene thermoplastic instead of the polydimethylsiloxane thermoset used in the present work.

3.3 Permittivity versus frequency

Beyond the nonlinear dependency of the conductivity with high electric fields, the effective use of a GnP-based composite as field grading material depends also on its losses. Indeed, if ohmic heating or dielectric losses become large, thermal runaway and subsequent breakdown may occur, limiting the use of this field grading material.

In the linear regime, the macroscopic Maxwell's curl equation for the magnetic vector field, $\mathbf{H}(\mathbf{r}, t)$, in a non-magnetic material is:

$$\boldsymbol{\nabla} \times \mathbf{H}(\mathbf{r}, t) = \frac{\partial D(\mathbf{r}, t)}{\partial t} + J_F$$

where J_F is the free current density ($J_F = \sigma E(r, t)$) and D is the electric displacement field $D = \varepsilon_0 \varepsilon E(r, t)$ where ε_0 is the vacuum permittivity, ε is the relative permittivity of the medium and σ its conductivity.

This gives:

$$\nabla \times \mathbf{H}(\mathbf{r},t) = \varepsilon_0 \frac{\partial \varepsilon\, \mathbf{E}(\mathbf{r},t)}{\partial t} + \sigma \mathbf{E}(\mathbf{r},t)$$

With time-harmonic vector fields of angular frequency ω ($\mathbf{H}(\mathbf{r},t) = \mathbf{H}(\mathbf{r})e^{j\omega t}$ and $\mathbf{E}(\mathbf{r},t) = \mathbf{E}(\mathbf{r})e^{j\omega t}$), one gets:

$$\nabla \times \mathbf{H}(\mathbf{r}) = j\omega\varepsilon_0\varepsilon_r'\mathbf{E}(\mathbf{r}) + (\varepsilon_0\varepsilon_r'' + \sigma(\omega))\mathbf{E}(\mathbf{r})$$

where ε_r' and ε_r'' are, respectively, the relative real and imaginary part of the permittivity ($\mathbf{H}(\mathbf{r})$ et $\mathbf{E}(\mathbf{r})$ are complex fields which may include a phase between them). The latter is the linear answer of the material to the applied electric field, meaning that it depends only on the frequency. Finally, the conductivity $\sigma(\omega) = \sigma_{DC}$ is assumed to be constant for the frequency range of interest.

Assuming that there are neither other loss mechanisms, nor mutual influence of the loss mechanisms, the complex relative dielectric permittivity can then be redefined as:

$$\varepsilon_r^* = \varepsilon_r' - j\,(\varepsilon_r'' + \frac{\sigma_{DC}}{\omega\varepsilon_0})$$

The dissipation or loss tangent:

$$\tan\delta_{total} = \tan\delta_{conductive} + \tan\delta_{dielectric} = \frac{\varepsilon_r'' + \frac{\sigma_{DC}}{\omega\varepsilon_0}}{\varepsilon_r'}$$

therefore, characterizes the total electrical dissipation.

A dielectric spectrum of a composite (45 wt.% GnP) is shown in **Fig. 7**. The dielectric constant decreases from 15 to 12 in the 10^{-2} – 10^{6} Hz range but is much higher than the neat polymer. This is significant considering the relative low filler fraction and the fact that GO-based nanocomposites have a typical permittivity of ~ 8 [33]. This high permittivity was already noted in GNPs nanocomposites aimed for electromagnetic interference (EMI) shielding applications (see [43]). It allows GnP-based composites to be used as capacitive field grading material. Meanwhile, the loss factor increases only moderately from 210^{-2} to 510^{-2} (**Fig. 7**) which indicates a low DC conductivity, though an order of magnitude higher than for GO-based nanocomposites.

For AC stress grading applications, the relevant function is the dependence of the permittivity ε_r' with the field. The permittivity (AC, f =50Hz) of the specimens as a function of the electric field has been extracted from the electrical characteristics. **Fig.8** shows a rise of the permittivity

above 3 wt.% which suggests a percolation threshold. It is also worth noting that the percolation is perceptible as it is for DC-resistivity.

4 Discussion

The origin of the nonlinear resistivity of the GNP composite is not straightforward. First let us note that a two-phase composite made of a polymer insulating host loaded with conductive fillers has to be above the percolation threshold to show a strong nonlinear resistivity behavior. Indeed, at low volume concentration, the conductivity of such a composite is mainly the result of transport processes occurring within the polymer matrix. It is only above the percolation, where the fillers are in close contact, that efficient conductive paths might appear. **Fig. 9** shows a transmitted light micrograph of the specimen loaded with 5 wt.% of graphite nanoplatelets. A multiscale microstructure is observed with the presence of micronic aggregates of nanoplatelets which may coexist with isolated primary nanoplatelets present in the grey background. Due to the large aspect ratio of GNP, percolation is therefore achieved at low filling fractions by aggregates-aggregates junctions involving or not isolated nanoplatelets. The origin of the electric change of the composites, observed above the critical filler volume fraction of about 3 vol.% (see **Fig. 5**), is then associated to a percolated microstructure. This might also explain why the switching field observed in our systems is two decades lower than the switching field observed in graphite nanoplatelets (GnP) in extruded low-density polyethylene [36,37]. Although the fillers content was similar (~1 and ~5%), the nanoplatelets were more dispersed in this system and, above all, strongly oriented by the extrusion **Fig. 10** illustrates the microstructures of an extruded and a randomly oriented nanocomposite when the concentration of the filler-loading increases. When the nanoplatelets are aligned (**Fig. 10 a**), the electrical conduction path remains blocked by layers of polymer matrix even at a large filler content. These layers restrict the rise of current with the increase of applied electric field E. Since the resistivity of the carbon filler is lower, a great part of applied voltage is transferred to the matrix

layer according to the voltage division rule. By contrast, a percolated microstructure forms rather easily with randomly oriented nanoplatelets (**Fig. 10 b**). The different microstructures explain the critical change in electrical resistivity with the field for the specimens of our study and the lack of percolation behavior in the case of extruded nanocomposites.

Percolation is necessary but not sufficient to provide an efficient nonlinear behavior in a two-phase composite. Two main mechanisms can be at the origin of nonlinear phenomena [44]. When conductive fillers remain separated by a thin layer of insulating polymer, the process of charge carrier transport can be controlled by tunneling/hopping [21]. This is the case of silicon carbide fillers for which the non-linearities stem from the contacts between particles [44]. On the other hand, the nonlinear behavior can be due to an intrinsic property of the particles as observed for ZnO microvaristors [44] or graphene oxide fillers [33]. The latter case is interesting since these fillers are also high aspect ratio carbonaceous particles Individual graphene oxide sheets are close-to-insulating because of the extensive presence of saturated sp^3 bonds and a high density of electronegative oxygen atoms bonded to carbon which give rise to an energy gap in the electron density of states (~ 2-10 Ωm [45]). However, chemical or thermal reduction results in a pronounced increase of conductivity (~3 orders). Partially reduced, individual graphene oxide sheets are characterized by a nonlinear current-voltage I(V) behavior [46] due to their heterogeneous microstructure. The 2D-sheets are made of sp^2 carbon clusters separated by amorphous and highly disordered sp^3 bonded regions This disrupted structure forms electrostatic barriers between the conductive sp^2 clusters and limit the charge transport inside the partially reduced GO individual sheets for an sp^2 fraction below 0.6, *i.e.* below 20 at.% oxygen [46]. The charge transport in individual partially reduced GO is space-charge-limited, the injected carriers in the individual sheet altering the local electric field created by the electrode potentials [47]. The electrons are indeed blocked by the energy barriers at low electric field and become capable of tunneling through them when the local electric field exceeds a specific local switching field which depends on the sp^2 clusters size, itself controlled

by the reduction rate of the GO sheet. The nonlinearity decreases as the reduction of the GO progresses [45,47] as a consequence of the increase of the sp^2 cluster size. At a sp^2 fraction of about 60% the sheets lose their nonlinearity behavior [46]. When such individual GO sheets are dispersed in a polymer matrix (at and above percolation) the composite conductivity is thought to be dictated by the motion of charge carriers within the sheets. The contacts between sheets do add only weak additional resistance, since conductivity within thin GO films have been shown to be not limited by junctions between the sheets [45].

In the case of GnP, some surface groups are present but they are mainly localized on the edge of the nanoplatelets. Moreover, their thickness is one order thicker than the GO sheets (11 nm [33]), and surface oxide groups such as carbonyl groups [36,45, 47-48] are far less abundant. The linear resistivity through and in-plane are 10^{-2} and 10^{-7} Ωm respectively [36], suggesting a large amount of delocalized π electrons available. The mechanisms invoked for GO sheets are therefore not relevant here for the GnP/silicone composites. It is therefore very likely that contacts between GnP aggregates or contact between aggregate and isolated primary of the multiscale organization possess a distribution of characteristic voltages above which the electrons can tunnel through.

5 Conclusions

We have examined the electrical behavior of graphite nanoplatelets filled silicone composites. They are found to possess nonlinear resistive field grading behavior with a resistivity-concentration dependence typical of percolated composites. For filler concentration below the percolation threshold, the resistivity of composites is found higher than pristine silicone matrix. GnP-Polymer interface barriers then hinder the charge movement of impurities ions within the host matrix. At about 4 wt.% of nanofillers, a field-dependent conductivity variation of 6 orders of magnitude is observed. GnP composites show similar properties than GO-based nanocomposites but the transition is less sharp and the switching field 2 orders of magnitude

lower. The nonlinear properties are interpreted as the result of a percolated or density (closed neighbors) microstructure made of the coexistence of aggregates and single nanoplatelets where the inter-platelet junction resistances are responsible of the macroscopic nonlinear behavior. After percolation threshold, further increase in the volume fraction does not result in any distinct change of the resistivity which agrees well with the behavior of composites filled with percolated semi-conductive fillers. At low field, composites of graphite nanoplatelets exhibit one order higher resistivity compared to the pristine polymer matrix, a significant dielectric constant of about 13 at 50 Hz associated to a loss factor of only 0.01. All these characteristics render the GnPs/silicone composites quite suitable materials for field grading materials.

Acknowledgements

The authors appreciate the financial supports provided by Occitanie Prematuration 2017 Tension 006684 ESR_PREMAT-000021. Some characterizations/experiments/measurements were performed with the support of the Balard Plateforme d'Analyses et de Caractérisation (PAC Balard). The authors thank Amine Geneste (PAC Balard) for technical support/assistance for the electrical measurements.

Declaration

Conflict of interest

The authors declare no conflict of interest.

References

1. T. Christen, L. Donzel, G. Greuter, Nonlinear Resistive Electric Field Grading Part 1: Theory and Simulation. IEEE Electrical Insulation Magazine 26(6), 47-59 (2010). doi: 10.1109/MEI.2010.5599979

2. C. Liu, Y. Zheng, B. Zhang, X. Zheng, S. Hu, K. Han, Review of Nonlinear Conductivity Theory. Research of Modified Composite Materials IEEE Access 7, 50536-50548 (2019). doi: 10.1109/ACCESS.2019.2906662

3. G. Mazzanti, J. Castellon, G. Chen, J.C. Fothergill, M. Fu, N. Hozumi, J.H. Lee, L. Li, T. Marsinotto, F. Fauseth, P. Morshuis, C. Reed, I. Troia, A. Tzimas, K. Wu, The Insulation of HVDC Extruded Cable System Joints. Part 1: Review of Materials, Design and Testing Procedures IEEE Transactions on Dielectrics and Electrical Insulation 26(3), 964-972 (2019). doi: 10.1109/TDEI.2019.007916

4. H. Ye, T. Fechner, X. Lei, Y. Luo, M. Zhou, Z. Han, H. Wang, Q. Zhuang, R. Xu, D. Li, Review on HVDC cable terminations. IET journals, The institution of Engineering and Technology - High Voltage 3(2), 79-89 (2018). doi: 10.1049/hve.2017.0144

5. H. Hourdequin, L. Laudebat, M. Locatelli, P. Bidan, Contribution à la conception de structures de packaging pour les modules de puissance très haute tension : contraintes sur les isolants. Symposium de génie électrique : EF-EPF-MGE-2016, 7-9 Juin 2016, Grenoble, France

6. C. Li, C. Lin, J. Hu, L. Weidong, Q. Li, B. Zhang, S. He, Y. Yang, F. Liu, J. He, Novel HVDC Spacers by Adaptively Controlling Surface Charges-Part I: Charge Transport and Control Strategy. IEEE Transactions on Dielectrics and Electrical Insulation 25(4), 1238 - 1247 (2018). doi: 10.1109/TDEI.2018.007054

7. A. Naeini, E. Cherney, S. Jayaram, Modified Stress Grading System for a 13.8 kV Inverter-Fed Rotating Machine. IEEE Transactions on Dielectrics and Electrical Insulation 26(4),1261-1266 (2019). doi: 10.1109/TDEI.2019.007991

8. C. Staubach, T. Hildinger, A. Staubach, Comprehensive electrical and thermal analysis of the stress grading system of a large hydro generator. IEEE Electrical Insulation Magazine 34(1):37-42 (2018). doi: 10.1109/MEI.2018.8246120

9. U. Patel, Jayaram S (2012) Impact of poor power quality on stress grading system of cable termination, Annual Report Conference on Electrical Insulation and Dielectric Phenomena, 14-17 Oct 2012. doi : 101109/CEIDP20126378820

10. X. Zhu, Y. Wang, Y. Zhang, J. Wu, Y. Yin, Harmonics in SiC/Alkyd Resin Composites with Different SiC Particle Sizes under Different Temperatures. IEEE Transactions on Dielectrics and Electrical Insulation 26(4):1350-1357 (2019). doi: 10.1109/TDEI.2019.008055

11. A. Can-Ortiz, L. Laudebat, Z. Valdez-Nava and S. Diaham, Nonlinear Electrical Conduction in Polymer Composites for Field Grading in High-Voltage Applications: A Review, Polymers 13, 1370, 1-58 (2021). doi.org/10.3390/polym13091370

12. S. Blatt, V. Hinrichsen, Mathematical Model for Numerical Simulation of Current Density in Microvaristor Filled Insulation Materials. IEEE Transactions on Dielectrics and electrical Insulation 12(2):1161-1170 (2015). doi: 10.1109/TDEI.2014.004740

13. D. Weida, C. Richter, M. Clemens, Design of ZnO Microvaristor Material Stress-cone For Cable Accessories. IEEE Transactions on Dielectrics and Electrical Insulation18(4),1262-1267 (2011). doi: 10.1109/TDEI.2011.5976125

14. R. Abd-Rahman, A. Haddad, N. Harid, H. Griffiths, Stress Control on Polymeric Outdoor Insulators Using Zinc Oxide Microvaristor Composites. IEEE Transactions on Dielectrics and Electrical Insulation 19(2):705-713 (2012). doi:10.1109/TDEI.2012.6180266

15. H. Ahmad, A. Haddad, H. Griffiths, S. Robson, T. Nishimura, N. Tsukamoto, Electrical characterisation of ZnO microvaristor materials and compounds. IEEE Conference on Electrical Insulation and Dielectric Phenomena (CEIDP):688-692 (2015) 10.1109/CEIDP.2015.7352035

16. L. Donzel, M. Montenegro-Uratsun, M. Hagemeister, P. Rukwid, ZnO stress grading tape for stator windings for electrical machines located at higher altitudes. Cigré 2016 D1-107: 1-12 (2016)

17. X. Zhao, X. Yang, J. Hu, H. Yang, Q. Li, J. He, Grading of Electric Field Distribution of AC Polymeric Outdoor Insulators Using Field Grading Material. IEEE Transactions on Dielectrics and Electrical Insulation 26(4), 1253-1260 (2019). doi: 10.1109/TDEI.2019.007989

18. X. Yang, J. Hu, J. He, Adjusting nonlinear characteristics of ZnO-silicone rubber composites by controlling filler's shape and size. IEEE International Conference on Dielectrics (ICD) 1, 313-317 (2016). doi:10.1109/ICD.2016.7547607

19. B.R.Varlow, J. Robertson, K.P. Donnelly, Nonlinear fillers in electrical insulating materials. IET Science, Measurement & Technology 1(2):96-102 (2007). doi:10.1049/iet-smt:20060007

20. Z. Li, Z. Yang, Y. Xing, W. Zhu, J. Su, X. Kong, J. Jiang, B. Du, Improving the Electric Field Distribution in Stress Cone of HTS DC Cable Terminals by Nonlinear Conductive Epoxy/ZnO Composites. IEEE Transactions on Applied Superconductivity 29(2), 7000305 (2009). doi: 10.1109/TASC.2018.2889357

21. X.Wang, J.K. Nelson, L.S.Schadler, H. Hillborg, Mechanisms Leading to Nonlinear Electrical Response of a Nano p-SiC/Silicone Rubber Composite. IEEE Transactions on Dielectrics and Electrical Insulation 17(6),1687-1696 (2010). doi: 10.1109/TDEI.2010.5658218

22. E. Mårtensson, U. Gäfvert, A three-dimensional network model describing a non-linear composite material. Journal of Physics D: Applied Physics 37(1), 112-119 (2004). doi: 10.1088/0022-3727/37/1/019

23. F. Wang, P. Zhang, M. Gao, X. Zhao, J. Gao, Research on the Non-linear Conductivity Characteristics of Nano-SiC Silicone Rubber Composites. Annual Report Conference on Electrical Insulation and Dielectric Phenomena, 535-538 (2013). doi : 10.1109/CEIDP.2013.6748326

24. A. Merouchi, E. David, F. Baudoin, D. Mary, I. Fofana, Optimization of the Electrical Properties of Epoxy- SiC Composites for Stress-Grading Application. IEEE Conference on Electrical Insulation and Dielectric Phenomena (CEIDP) 713-716 (2015). doi: 10.1109/CEIDP.2015.7352140

25. B.X. Du, Z.L. Li, Z.R. Yang, Field-dependent Conductivity and Space Charge Behavior of Silicone Rubber/SiC Composites. IEEE Transactions on Dielectrics and Electrical Insulation 23(5), 3108-3116 (2016) doi: 10.1109/TDEI.2016.005768

26. B.X. Du, Z.R. Yang, Z.L. Li, J. Li, IEEE Transactions on Dielectrics and Electrical Insulation 24(3):1340-1348 (2017). doi: 10.1109/TDEI.2017.006137

27. L.S. Schadler, X. Wang, J.K. Nelson, H. Hillborg, Dielectric Polymer Nanocomposites J Keith Nelson Editor 259 (2010). doi: 10.1007/978-1-4419-1591-7

28. L.X. He, S.C. Tjong, Zener tunneling in conductive graphite/epoxy composites: Dielectric breakdown aspects. Express Polymer Letters 7(4), 375-382 (2013). doi: 10.3144/expresspolymlett.2013.34

29. Q. Liu, X. Yao, X. Zhou, Z. Qin, Z. Liu, Varistor effect in Ag–graphene/epoxy resin nanocomposites. Scripta Materialia 66(2), 113-116 (2012) doi:10.1016/j.scriptamat.2011.10.016

30. Y. Yuan, Z. Qu, Q. Wang, E. Cheng, X. Sun, The Nonlinear I–V Behavior of Graphene Nanoplatelets/Epoxy Resin Composites Obtained by Different Processing Methods. Journal of Inorganic and Organometallic Polymers and Materials 29, 1198 (2019) doi:10.1007/s10904-019-01083-6

31. H. Lin, W. Lu, G. Chen, Nonlinear DC conduction behavior in epoxy resin/graphite nanosheets composites. Physica B: Condensed Matter 400(1), 229-236 (2007). doi:10.1016/j.physb.2007.07.015

32. Y. Yuan, Q. Wang, Z. Qu, Nonlinear DC Conduction Behavior in Graphene Nanoplatelets/Epoxy Resin Composites. IOP Conference Series: Materials Science and Engineering 301(1), 012015 (2018). doi:10.1088/1757-899X/301/1/012015

33. Z. Wang, J.K. Nelson, H. Hillborg, S. Zhao, L.S. Schadler, Graphene Oxide Filled Nanocomposite with Novel Electrical and Dielectric Properties. Advanced Materials 24(23), 3134-3137 (2012). doi: 10.1002/adma.201200827

34. Z. Wang, J.K. Nelson, H. Hillborg, S. Zhao, L.S. Schadler, Nonlinear Conductivity and Dielectric Response of Graphene Oxide Filled Silicone Rubber Nanocomposites. Annual Report Conference on Electrical Insulation and Dielectric Phenomena 40-43 (2012). doi: 10.1109/CEIDP.2012.6378717

35. W. Li, U.W. Gedde, H. Hillborg, Structure and Electrical Properties of Silicone Rubber filled with thermally Reduced Graphene Oxide. IEEE Transactions on Dielectrics and Electrical Insulation 23(2),1156-1163 (2016). doi: 10.1109/TDEI.2015.005485

36. K. Gaska, X. Xu, R. Kádár, B. Ganjipour, A.Yurgens, S. Gubanski, Influence of manufacturing process on electrical properties of LDPE-GnP nanocomposites. Proceedings of the Nordic Insulation Symposium 25 (2017)

37. G. Xu, S. Gubanski, R. Kádár, Electrical, Mechanical, and Thermal Properties of LDPE Graphene Nanoplatelets Composites Produced by Means of Melt Extrusion Process. Polymers 9(1):1-12 (2017). doi:10.3390/polym9010011

38. R. Metz, C. Blanc, S. Dominguez, S. Tahir, R. Leparc, M. Hassanzadeh, Nonlinear field dependent conductivity dielectrics made of graphite nanoplatelets filled composites, Materials Letters 292:129611 (2021). doi:10.1016/j.matlet.2021.129611

39 ASTM D257-14 Standard Test Methods for DC Resistance or Conductance of Insulating Materials, ASTM International, Subcommittee : D0912, West Conshohocken, PA (2014)

40. H. Takao, M. Okoshi and N. Inoue, Swelling and modification of silicone surface by F2 laser irradiation, Appl. Phys. A, Materials Science & Processing, 79, 1571-1574 (2004)

41. M. Wåhlander, F. Nilsson, R.L. Andersson, A. Carlmark, H. Hillborg, E. Malmström, Reduced and Surface-Modified Graphene Oxide with Nonlinear Resistivity. Macromolecular Rapid Communications 38(16), 1700291 (2017). doi: 10.1002/marc.201700291

42. S. Diaham, E. Pizzutilo, L. Da Gama Fernandes Vieira, Z. Valdez Nava, J.Y. Chane Ching, E. Flahaut, D. Fabiani, Novel Electrical Conduction Properties Obtained in Few-Layer Graphene/Epoxy Nanocomposites. IEEE International conference on Nanotechnology 27-30, 472-475 (2015). doi : 10.1109/NANO.2015.7388640

43. A. H. Kumar, M. B. Ahamed, K. Deshmukh, M. S. Sirajuddeen, Morphology, Dielectric and EMI Shielding Characteristics of Graphene Nanoplatelets,Montmorillonite Nanoclay and Titanium Dioxide Nanoparticles Reinforced Polyvinylidenefluoride Nanocomposites. Polym. Mater. 31, 2003-2016 (2021). doi:10.1007/s10904-020-01869-z

44. L. Donzel, F. Greuter, T. Christen, Nonlinear Resistive Electric Field Grading Part 2: Materials and Applications. IEEE Electrical Insulation Magazine 27 (2), 18-29 (2011). doi: 10.1109/MEI.2011.5739419

45. C. Gómez-Navarro, R.T. Weitz, A.M. Bittner, M. Scolari, A. Mews, M. Burghard and K. Kern , Electronic Transport Properties of Individual Chemically Reduced Graphene Oxide Sheets. Nano Letters 7 (11), 3499–3503 (2007). doi : 10.1021/nl072090c

46. C. Mattevi, G. Eda, S. Agnoli, S. Miller, K.A. Mkhoyan, O. Celik, D. Mastrogiovanni, G. Granozzi, E. Garfunkel, M. Chhowalla, Evolution of Electrical, Chemical, and Structural Properties of Transparent and Conducting Chemically Derived Graphene Thin Films. Adv Funct Mater 19, 2577–2583 (2009). doi: 10.1002/adfm.200900166

47. I. Jung, D. Dikin, R. Piner, R. Ruoff, Tunable Electrical Conductivity of Individual Graphene Oxide Sheets Reduced at “Low” Temperatures. Nano Lett (12), 4283-4287 (2008). doi: 10.1021/nl8019938

48. B. Ghavami, A. Rastkar-Ebrahimzadeh, Varistor characteristics of a nano-device containing graphene and oxidised graphene: verification by DFT + NEGF. Molecular Physics 113(23), 1-7 (2015). doi:10.1080/00268976.2015.1053549

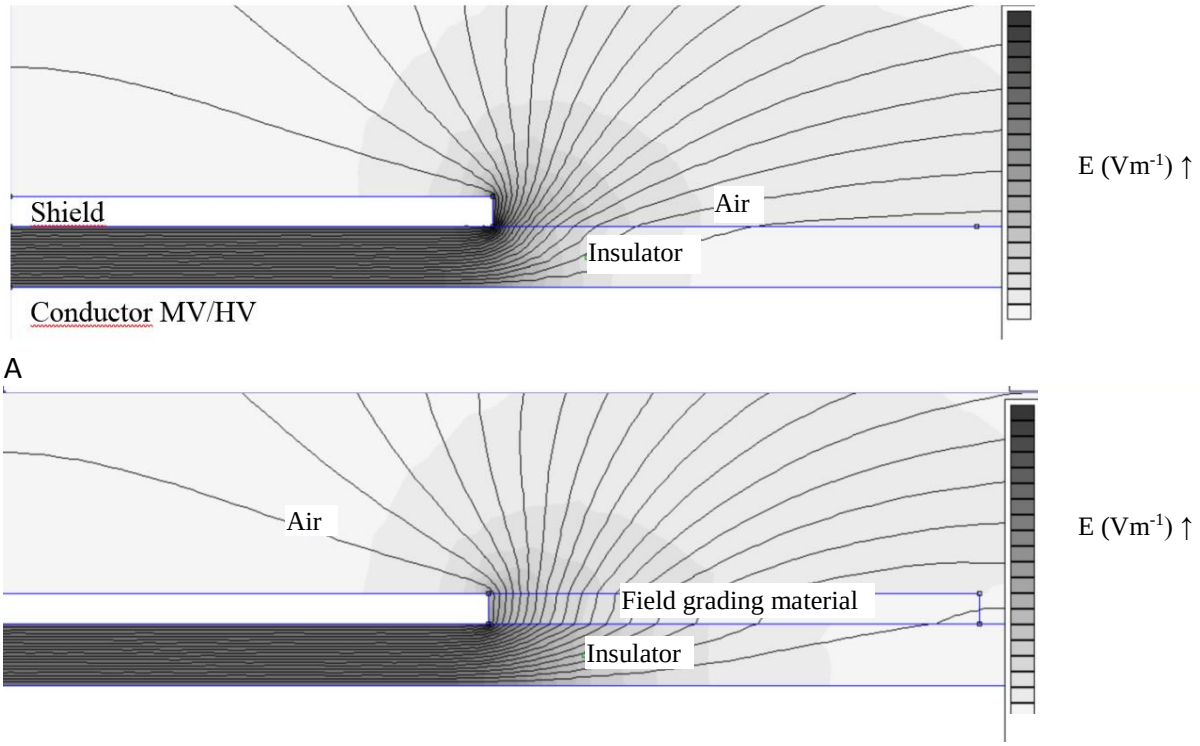

Fig.1. (A) Equipotential lines and electric field intensity near a shielded cable termination. Electric field may reach critical values near the end of the shield as depicted by grey scale. B. A layer of nonlinear material coats the termination of the cable: the equipotential lines are scattered, leading to a field reduction in the vicinity of the shield/insulator/air.

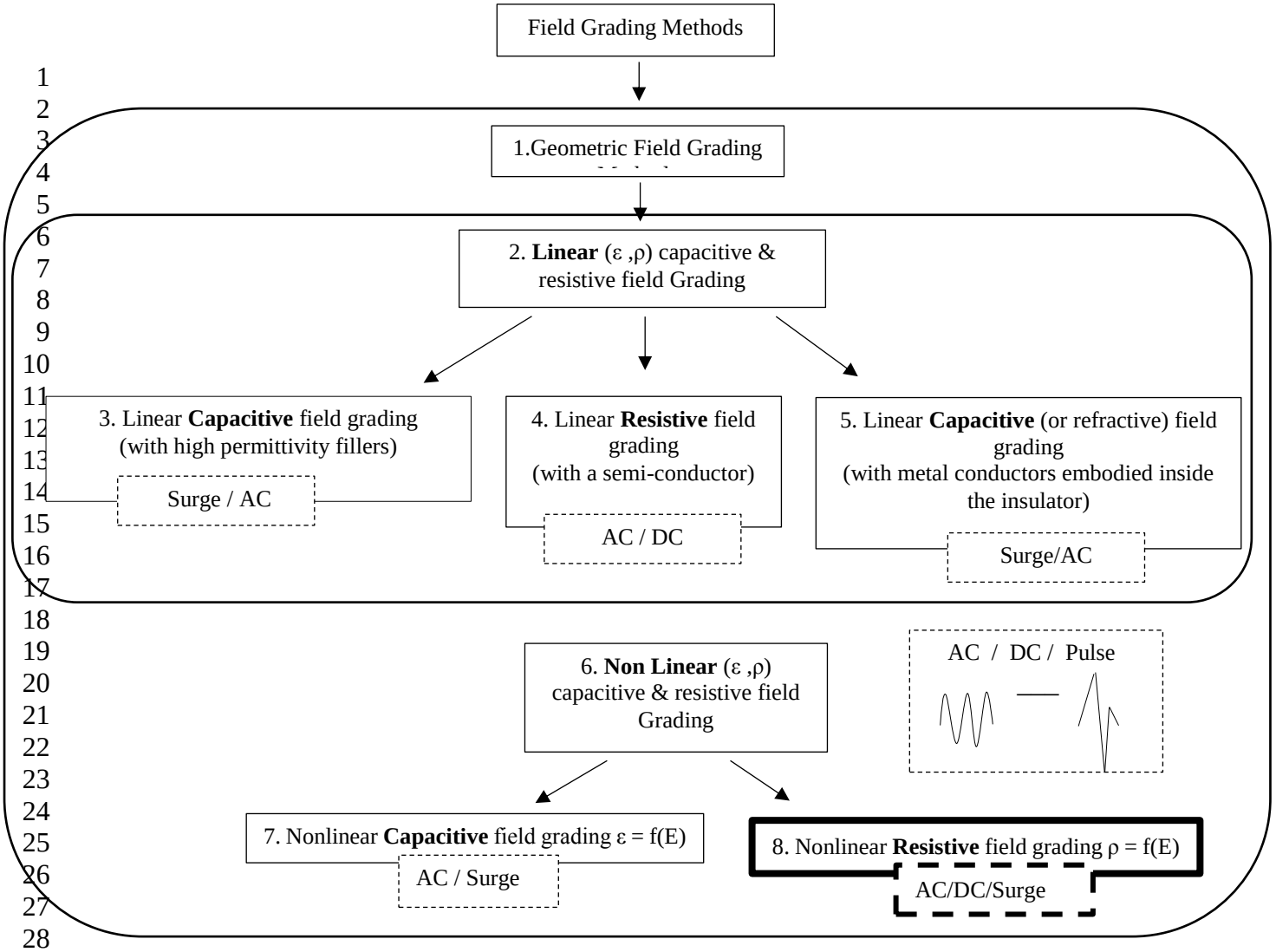

Fig.2. Schematic overview of some electric stress grading strategies to overcome flashovers and breakdown under AC, DC and imSurge conditions.

A

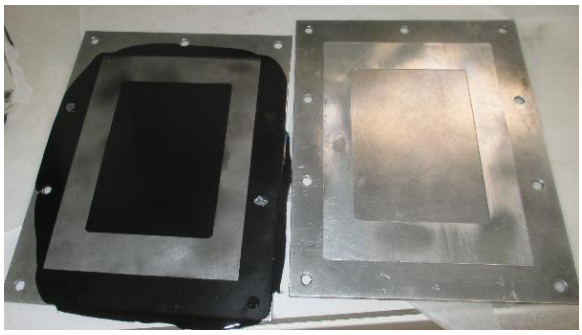

B

Fig. 3. (A) Electric heated platens for polymer composite plates production. (B) Resulting specimen after 150°C during 1 hour.

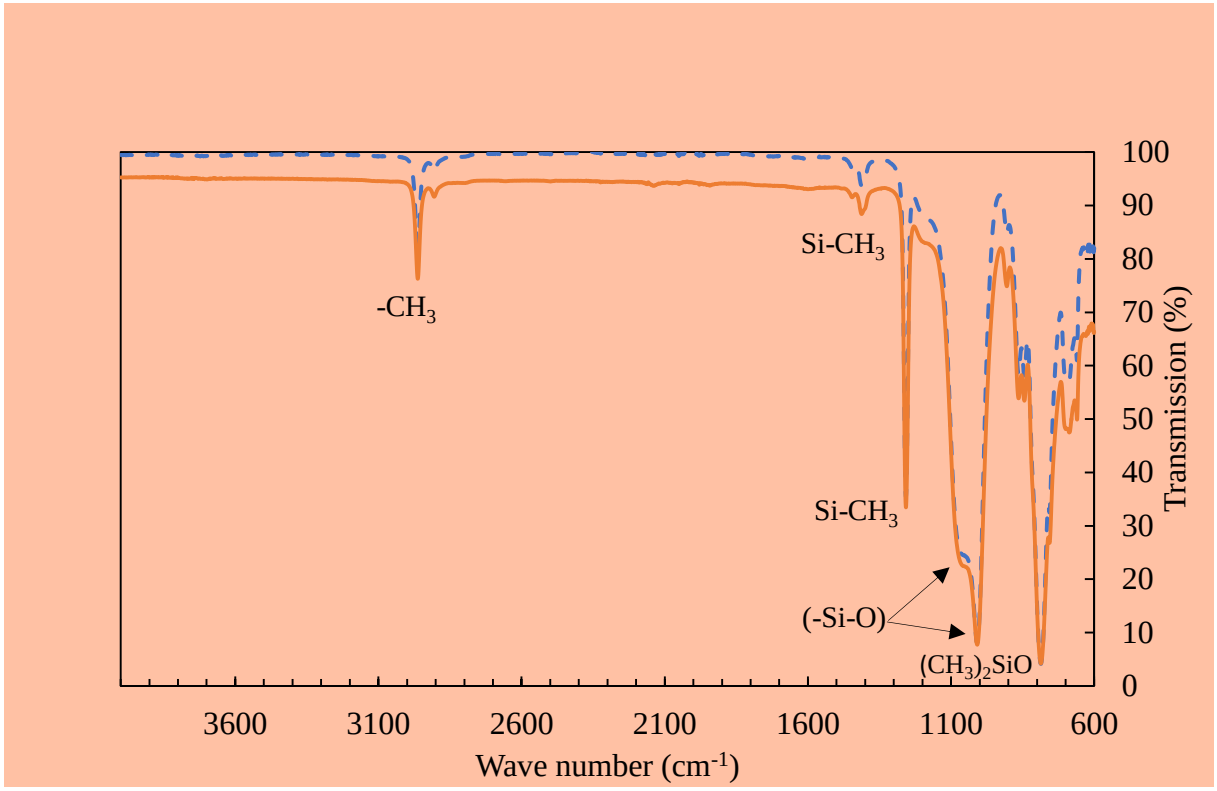

Fig. 4. ATR FT-IR spectra (Attenuated Total Reflection Fourier-transformed infrared) of the neat silicone (dash line) and 4 wt.% filled graphite nanoplatelets (hatched curve).

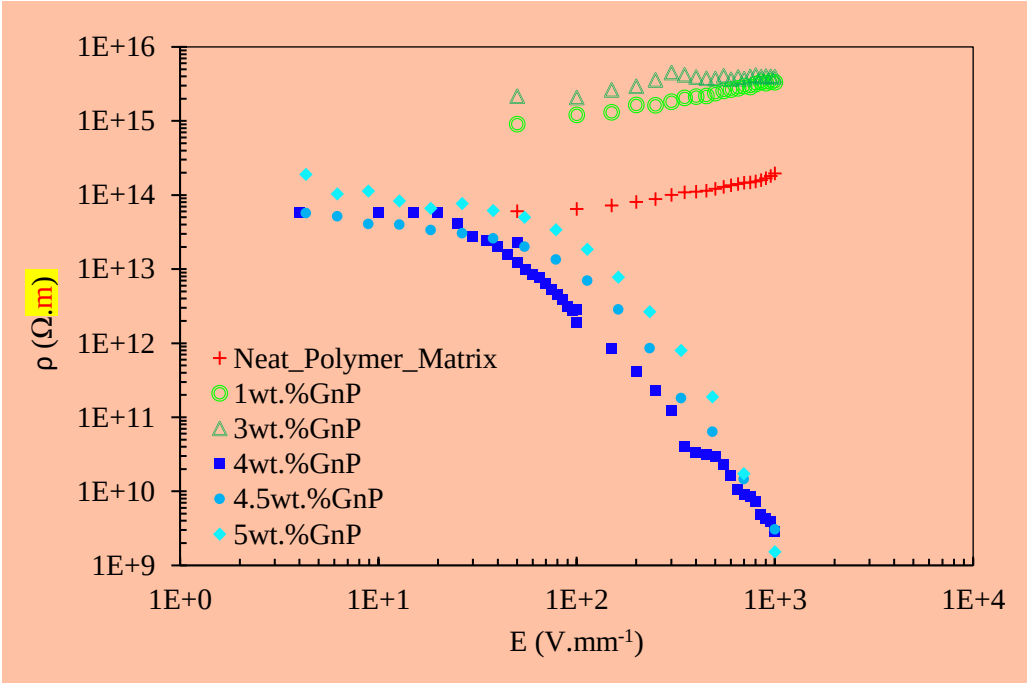

Fig. 5 Plot of resistivity with respect to field strength for GnP_based silicone composites with different loading of graphite nanoplatelets

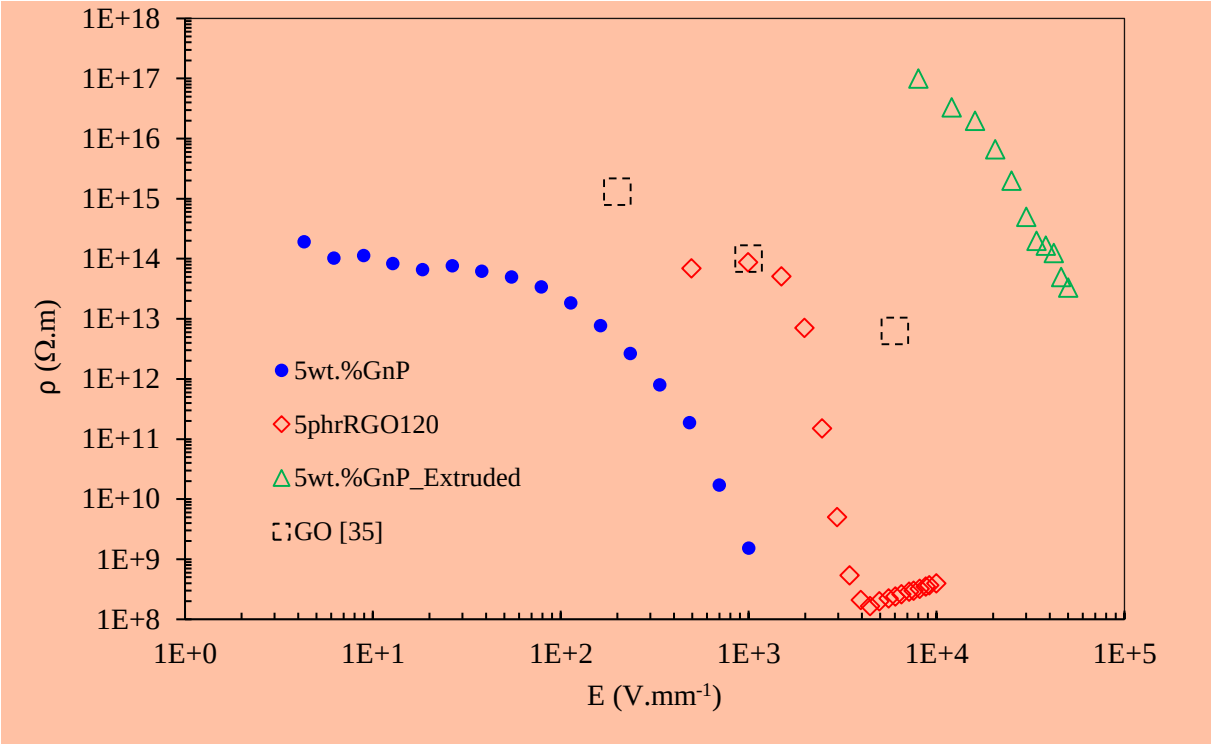

Fig. 6 Typical resistivity-field dependency of a GnP-based composite (5 wt.% GnP in silicone) compared with two series of samples from the literature: slightly thermally reduced graphene oxide at 120°C (empty diamonds) [32], GO/silicone composite filled at 3 wt.% [35] and GnP/polyethylene composite in a direction perpendicular to the extrusion direction at high field (empty triangles) [35]

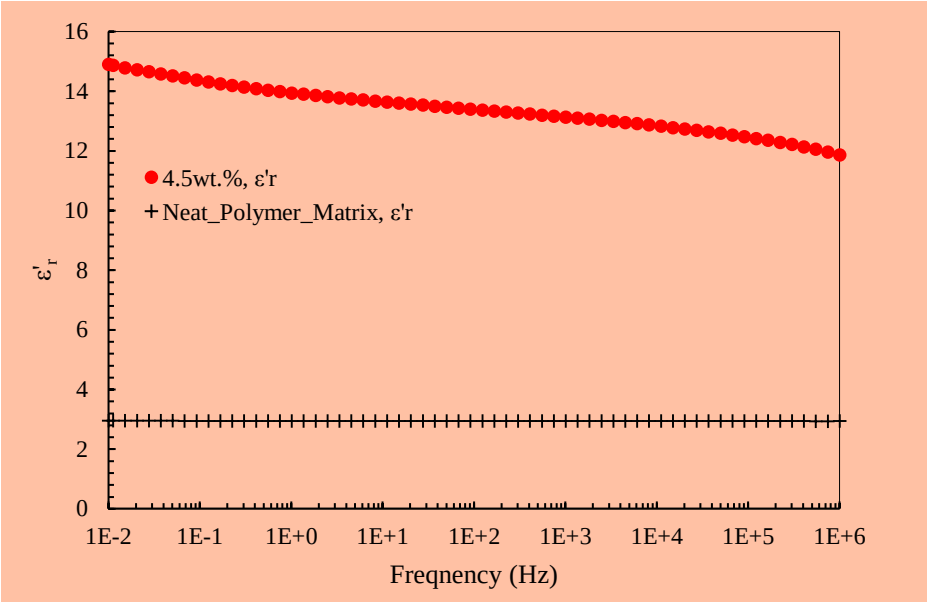

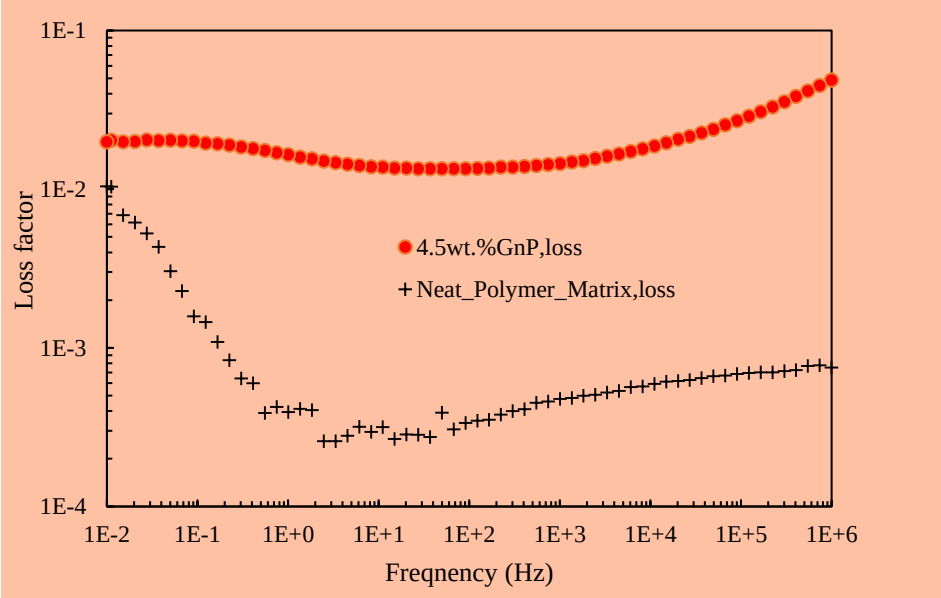

Fig. 7 Relative permittivity and dissipation factor (tan δ) spectrum at room temperature for the pure PDMS matrix and a 4.5 wt.% GnP /silicone nanocomposite

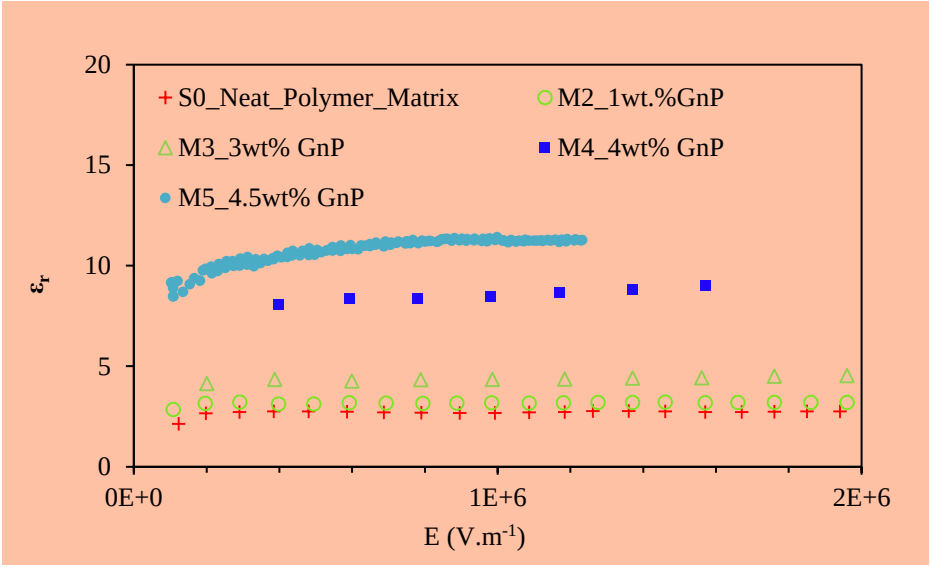

Fig. 8. Plot of the permittivity with respect to field strength for GnP based silicone composites with different loading of graphite nanoplatelets. (50 Hz

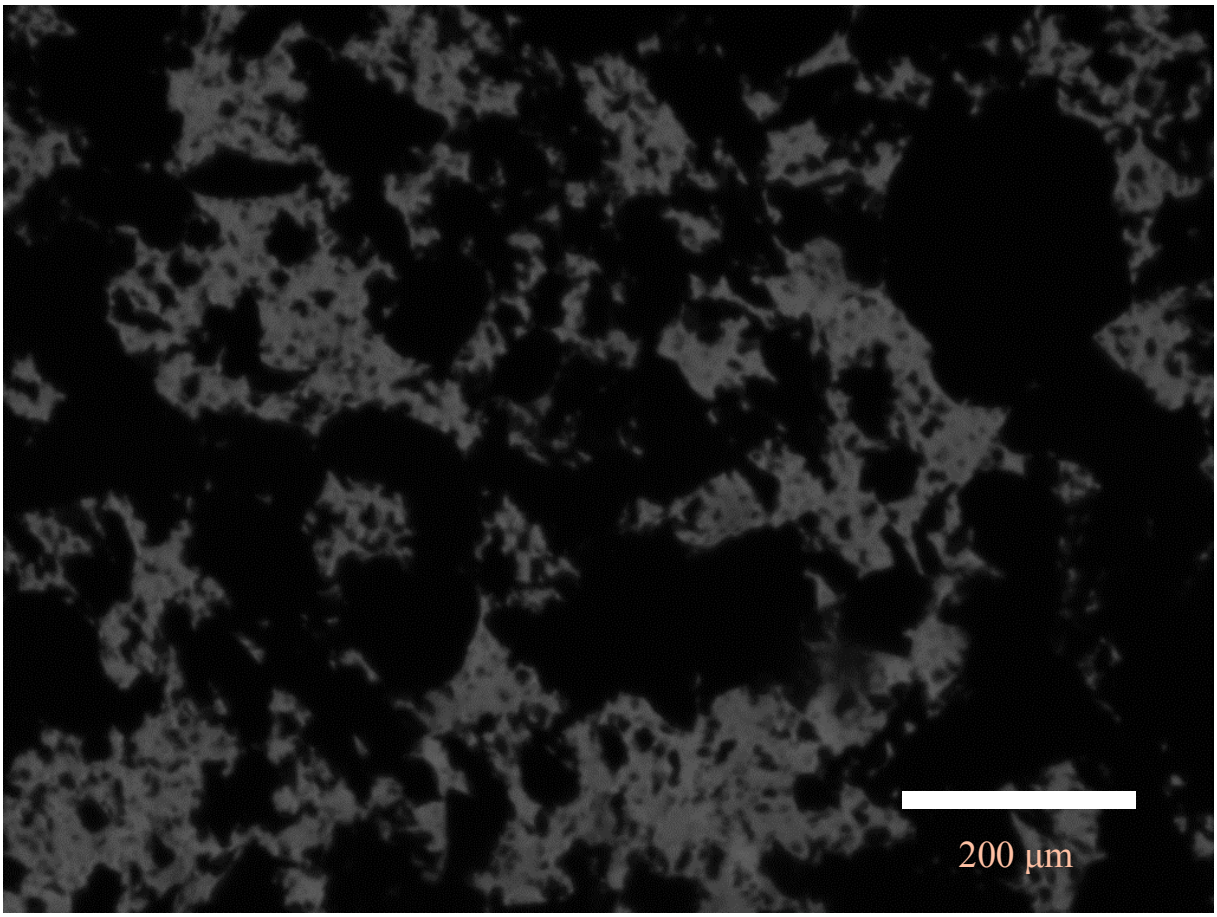

Fig. 9 Optical microscopy of the specimen with 5 wt.% of fillers. A multiscale microstructure with micronic aggregates is observed in a grey background filled of isolated primary nanoplatelets

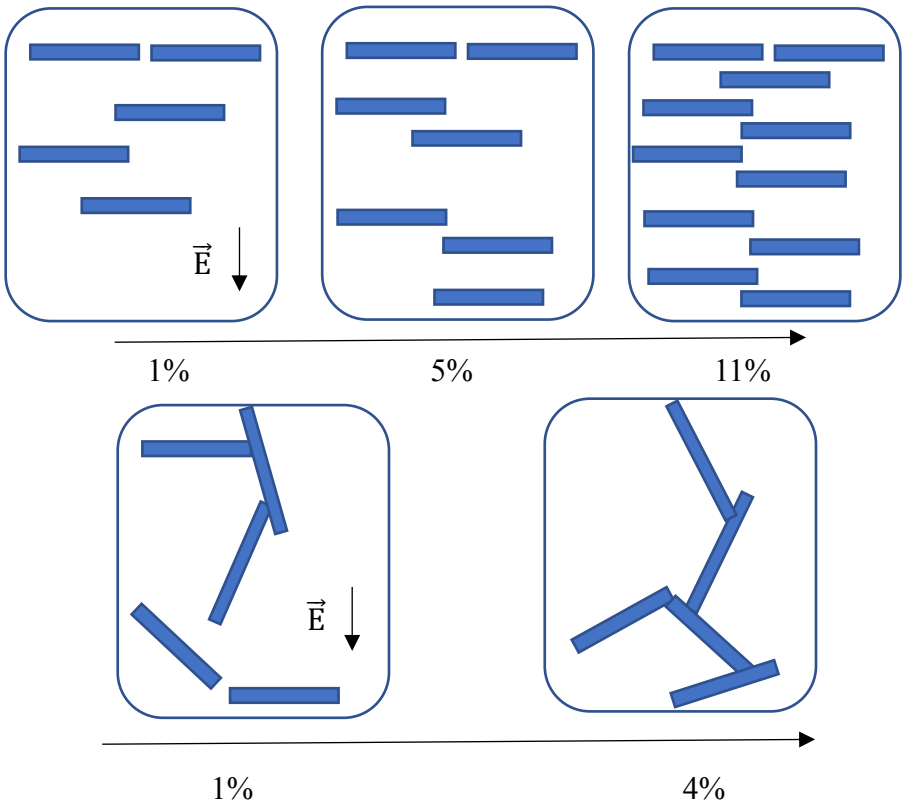

Fig. 10 Sketch of expected microstructure as a function of the volume concentration of the fillers for (A) extruded nanocomposites with nanoplatelets aligned in the direction of the extrusion flow and for (B) randomly oriented nanocomposites. (Electrical measurements are carried out perpendicular to the parallel filler alignment as depicted by the electric field vector $\vec{E}$)